HAMK
Häme University
of Applied Sciences

Anti-friction fifth-wheel brake system

Bachelor's thesis

Mechanical Engineering and Production Technology

Autumn2024

Alireza Safi Esfahani

HAMK
Häme University
of Applied Sciences

Degree Programme in Mechanical Engineering and Production Technology Abstract
Author Alireza safi esfahani Year 2024
Subject Anti-friction fifth wheel brake system
Supervisors Esa Murtola

This thesis presents the development and design of a novel brake mechanism, based on my patented invention (International Classification B60W 10/18; B60W 30/00; B60T 8/00). The research includes a dynamic analysis using D'Alembert's Principle, detailed stress analysis, and the intricate design of the braking system's components, capable of withstanding a braking acceleration of 15.5 m/s² the highest rate for racing cars. This performance is sufficient to stop a vehicle traveling at 110 km/h within a 30-meter braking distance for a car weighing up to 2000 kg.

A thorough study was conducted to assess the maximum stress and deformation on the mechanism’s parts, leading to the selection of appropriate materials and dimensions to ensure adequate strength. The 3D modeling was executed using SolidWorks a computer-aided design software program, with simulations performed in Abaqu a software suite for finite element analysis. The design adhered to established standards and utilized authoritative manufacturer catalogs.

The study concludes with a detailed design of the brake mechanism that meets stringent braking performance criteria, ensuring robustness and reliability under operational conditions, thereby enhancing vehicular safety. However, further investigation is needed for the helical rotor, as braking and its analysis require comprehensive research.

Keywords Braking system, Stress analysis, Detail design
Pages 48 pages and appendices 2 pages

Contents

Figures

Tables

Equations

Appendices

Appendix 1 Highway rule for typical stopping Distances (NHTSA ,2023)

Appendix 2 Braking Acceleration of different Types of Cars (Smith, J., & Johnson, 2023)

1 Introduction

In recent years, the need for advanced braking systems has become increasingly apparent due to Increased vehicle speeds and power. This thesis builds upon a patented invention (international classification B60W 10/18; B60W 30/00; B60T 8/00) that I developed in 2017. This thesis delves into the development and evaluation of braking mechanism, designed to substantially reduce the braking distance of vehicles, thereby enhancing automotive safety. The mechanism, mounted on the rear chassis of the vehicle and positioned between the rear tires, aims to improve braking performance by introducing a novel approach to braking dynamics.

The proposed braking mechanism is characterized by a main arm that deploys a wheel downward at the moment of braking and retracts it afterward. As depicted in Figures 1 and 2, two independent sets of the mechanism are installed between the car's rear tires. The primary components of the mechanism include a main arm, a hydraulic cylinder, and a wheel assembly. The wheel assembly itself comprises a rotating shaft, ball bearings, and a cylindrical shell ring covered by rubber (tire), which engages with the asphalt during braking.

Figure 1 The location of installation on car chassis

Figure 2 The brake system

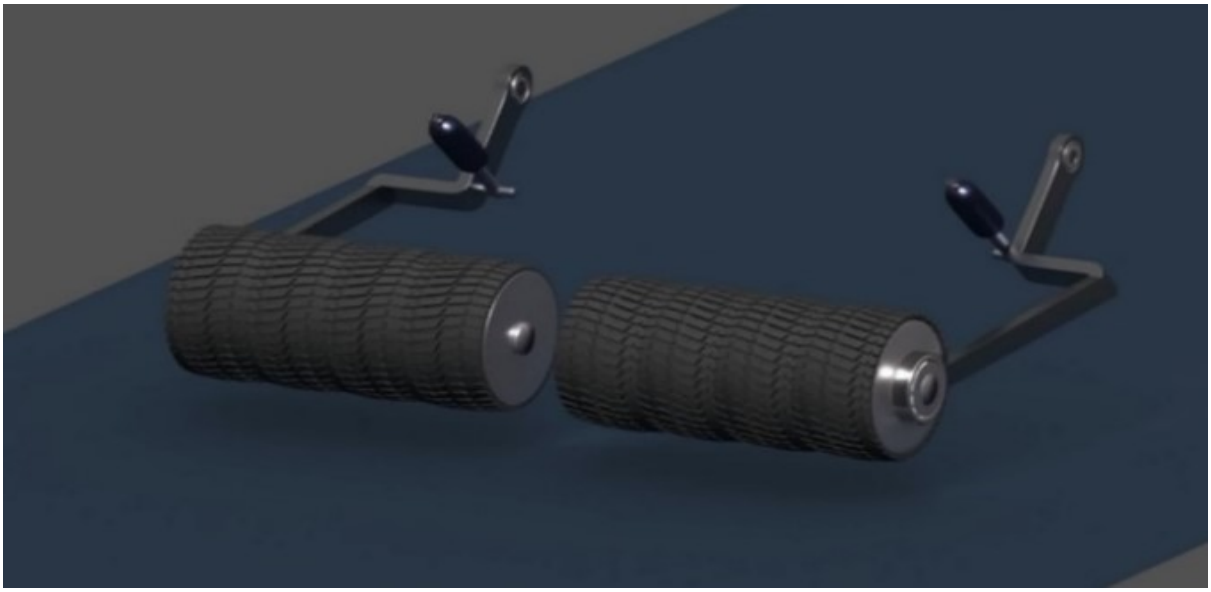

A detailed schematic of the mechanism's components is shown in Figure 2. The main arm is pivoted on the car chassis using a steel pin and is actuated by a hydraulic cylinder connected to the arm. The wheel shaft is mounted on the arm using ball bearings and an interference fit, ensuring smooth rotational motion. The hydraulic cylinder's end cap is securely attached to the car chassis, providing the necessary force to actuate the arm.

The primary goal of this project is to develop a 3D model of the braking mechanism, evaluate the stress and deformation characteristics of the mechanism and its components, and finalize the detailed design of each part. This includes selecting appropriate materials based on established standards to ensure durability and reliability under operational conditions.

To achieve these objectives, the research will employ the following method:

Using SolidWorks software, a detailed 3D model of the braking mechanism will be created. This model will serve as the basis for subsequent analysis and design refinement.

Using Abaqus software, Finite Element Analysis (FEA) will be employed to evaluate the stress distribution and deformation characteristics of the mechanism under various loading conditions. This analysis will help identify potential failure points and areas requiring reinforcement.

Based on the stress analysis results, appropriate materials will be selected for each component, ensuring compliance with relevant standards. The detailed design will be refined to optimize performance and durability.

The main goal of this study is to design components for a previously patented braking system idea. This thesis bridges the gap between theoretical analysis and practical application, developing a mechanism that not only meets stringent safety standards but also advances current braking technologies. Through careful design, analysis, and material selection, the research strives to enhance automotive braking performance.

2 Model Description

As shown in Figure 3, the model consists of a steel arm with a 3D sketch, featuring two bends in different planes. It is connected to the chassis and positioned between the rear wheels of the vehicle, although the exact placement may vary for different vehicles. The steel arm is connected to the hydraulic cylinder via revolute joints. Another side of the arm connects to the wheel shaft. The wheel consists of a shaft (with a helix plate welded on it), 2 disks a bearing mounted on the shaft, and a cylindrical steel shell ring and rubber (tire) that covers it.
Figure 3 shows the wheel designed in SolidWorks cross section and the wheel parts are visible. The total weight of the brake is about 20 kg.

Figure 3 Brake parts 3D-schematic from SolidWorks

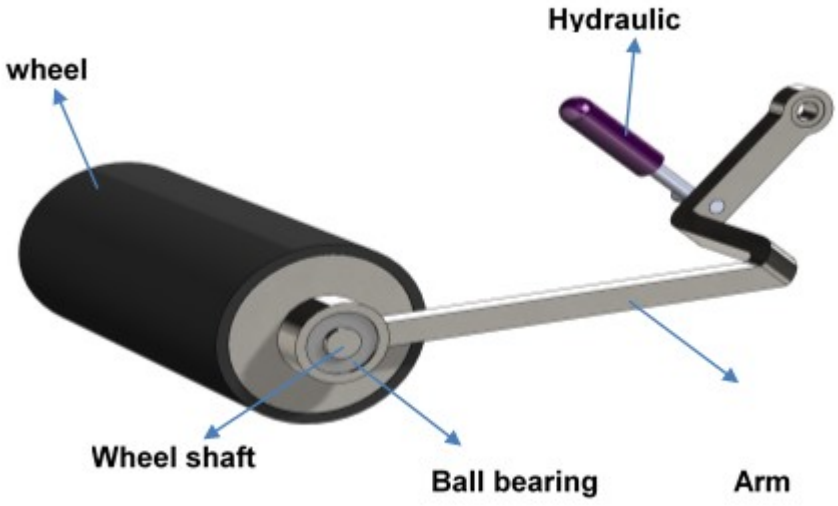

2.1 Mechanism location

The mechanism is fixed relative to the car chassis and during the braking time, the hydraulic cylinder keeps the wheel in contact with the ground (asphalt).

The dimensions may vary depending on different vehicles, but in this research, they have been selected based on the specific case being examined to ensure proper fit and functionality.

Dimensions and material properties that were assigned to the main part of the mechanism are shown in Figures 4 to 8 .all dimensions in figures are in millimeters.

Figure 4 Brake overall dimensions in millimeters

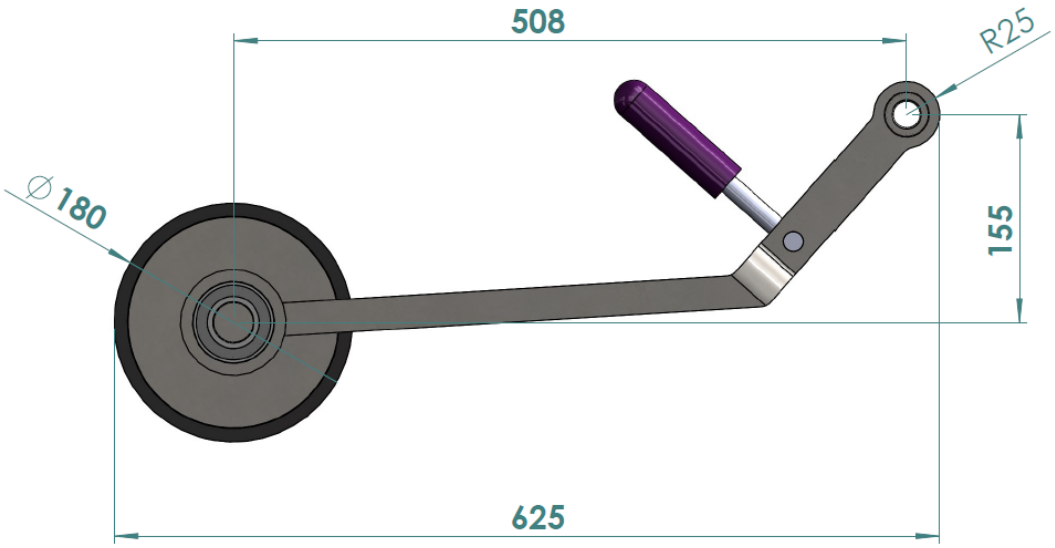

Figure 5 Brake wheel parts

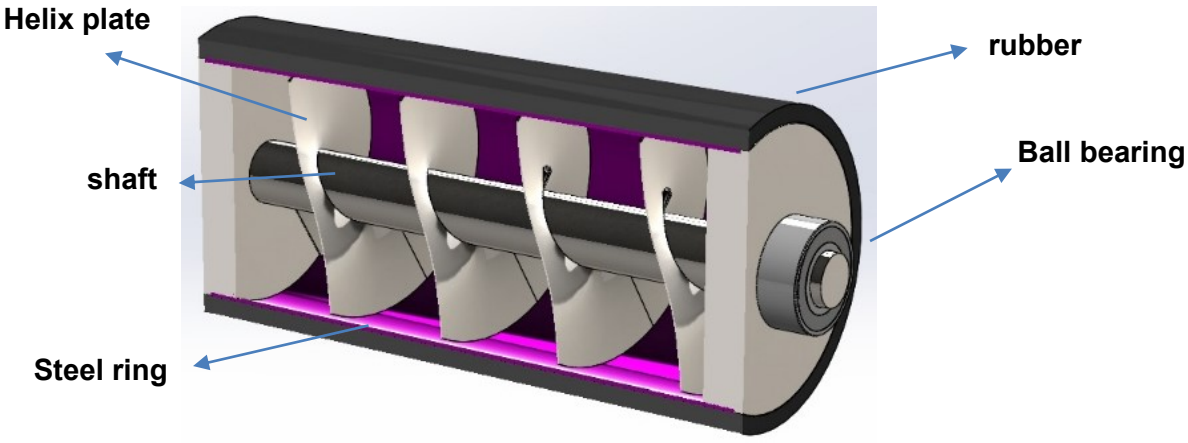

Figure 6 Arm dimensions in millimeters

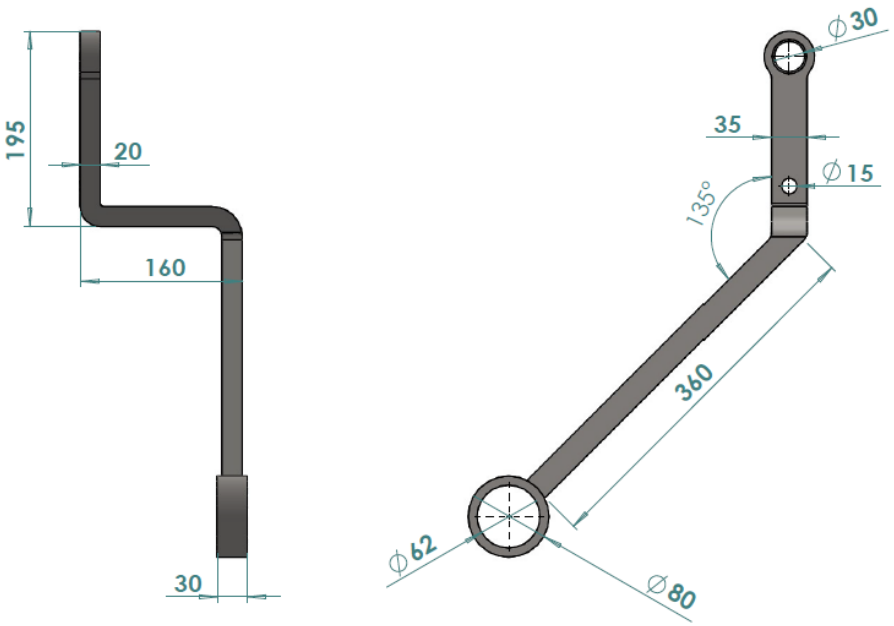

Figure 7 Wheel dimensions in millimeters

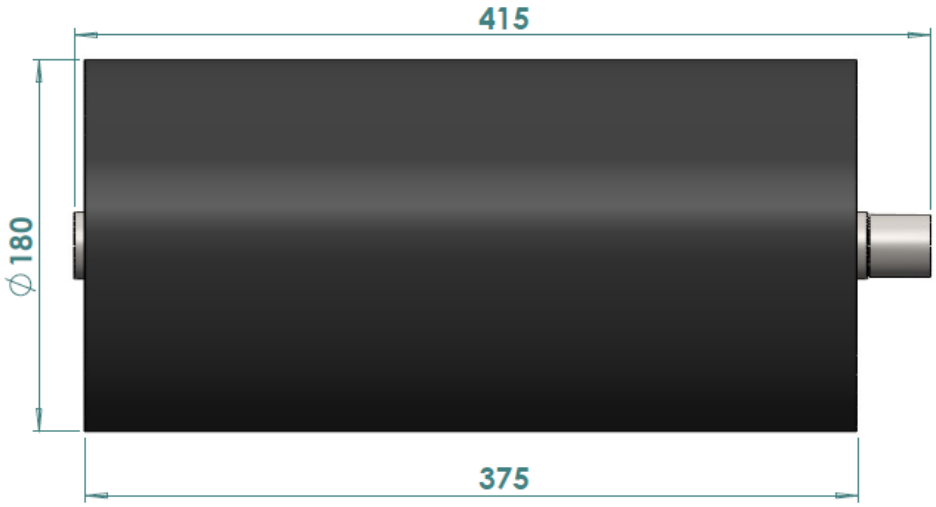

Figure 8 Shaft dimensions in millimeters

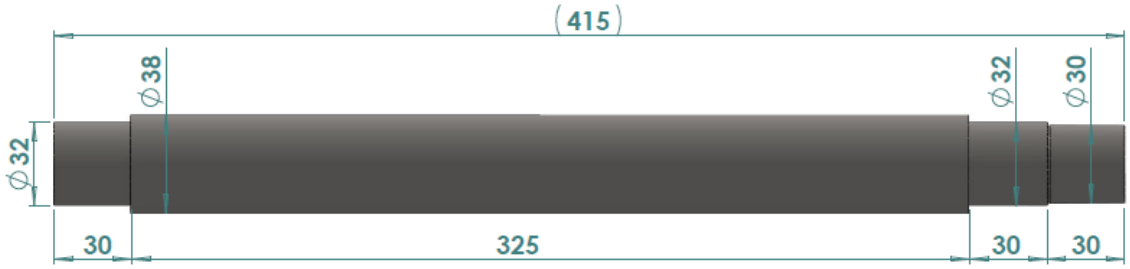

2.2 Free Body Diagram

Static equilibrium of the mechanism under the exerted forces has been considered. As shown in Figure 9, these forces include the normal reaction and rolling friction force from the ground to the wheel, the hydraulic force from the hydraulic cylinder, and the upper pin reaction forces.

Additionally, a simple dynamic model of the car during braking is necessary to calculate the maximum achievable normal reaction force (N) and, subsequently, the maximum static friction force (assuming pure rolling of the wheel) that can be applied to the brake mechanism.

Figure 9 Force diagram exerted on brake, dimensions in millimeters

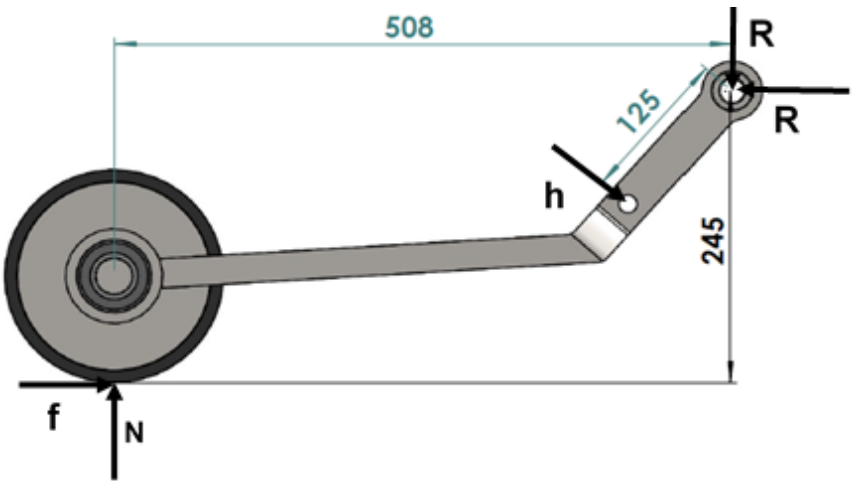

Figure 10 Dynamic model of car in braking time **(**Wright (1999-2005)**)**

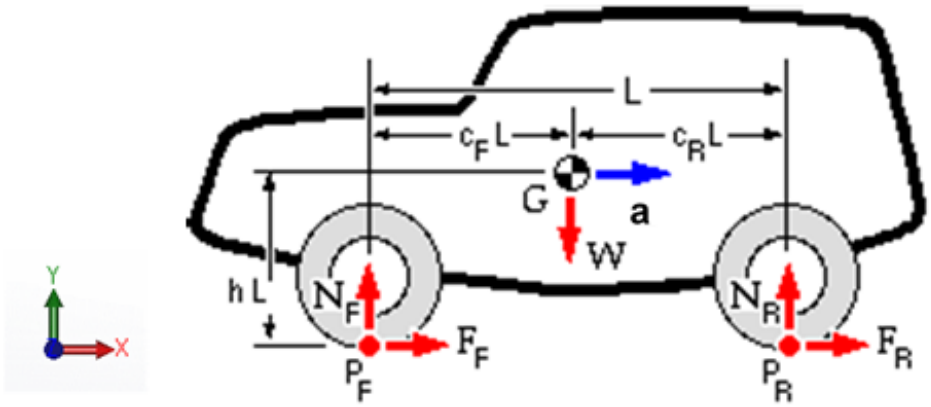

The required braking acceleration is approximately 15.5 m/s², which is the highest braking rate of racing cars, assuming constant acceleration motion. This rate is sufficient to stop a car traveling at 110 km/h within a 30-meter distance. The car's maximum allowable weight is 2000 kg. The required dimensions of the car are shown in Figure 11, with all dimensions in millimeters (Brembo**,**n.d.) .

Figure 11 The car overall dimensions(BMW, 2024).

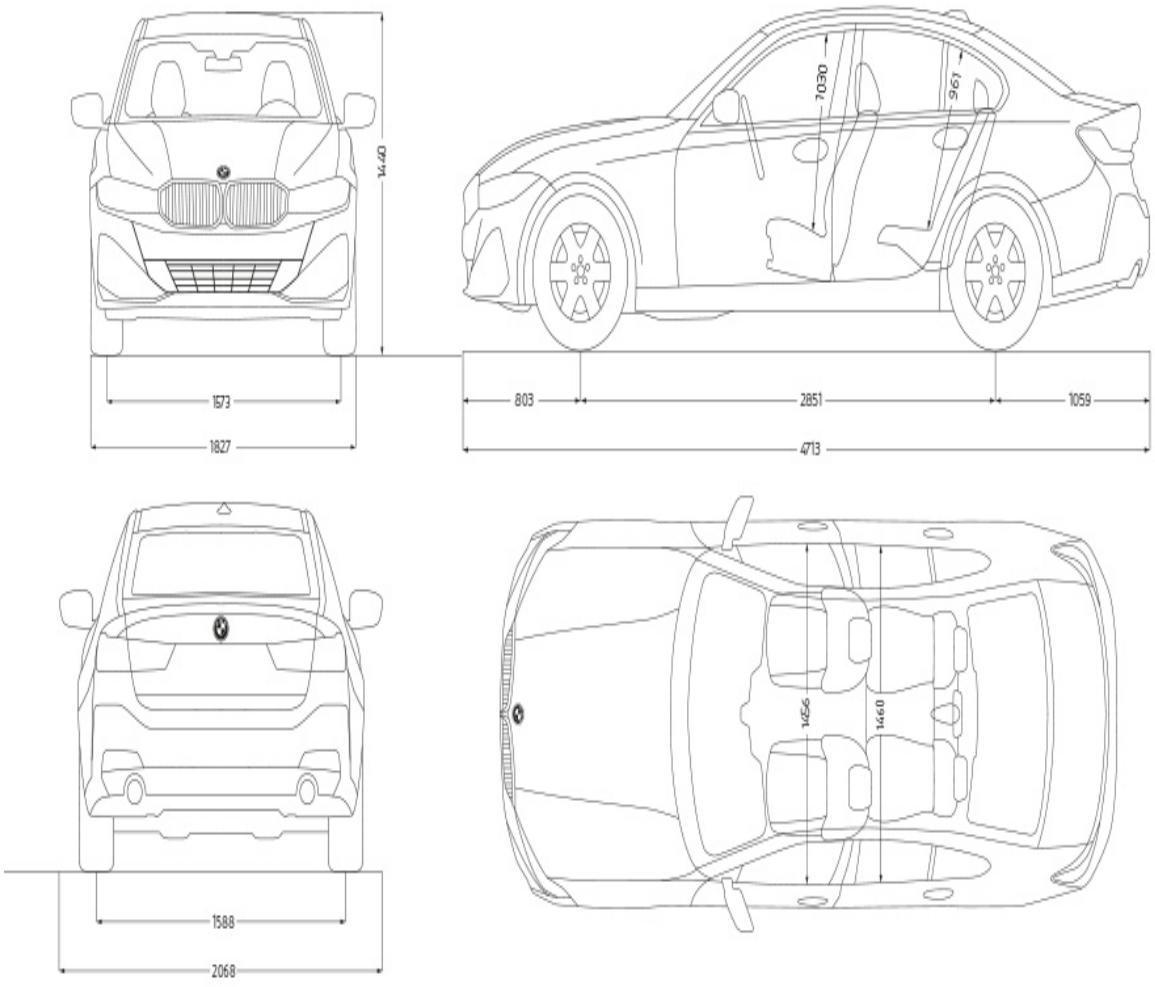

3 Analysis Methodology

The analysis includes 3 steps as below:

(2D) Rigid Body Model Dynamic Analysis

In this step, a simple dynamic analysis of the car will result from the maximum normal reaction and friction force (figure 10) that can be applied to the brake mechanism. Also, the maximum friction force in rolling conditions can be calculated. (Wang, J., & Zhang, C. 2021)

Applying previous step forces on the brake mechanism (figure 9)

The Forces N and f are Determined

So, by writing a static equilibrium on the mechanism in the system coordinate which is attached to the car chassis, the other forces in Figure 9 and detail design of the mechanism part can be evaluated.

Mechanism Analysis in ABAQUS Software

After detailed design in step 2, The parts 3D model was designed in SOLIDWORKS software and then imported into Abaqus for evaluating stress and deformation in parts and modifying dimensions or material of the parts.

4 Analysis Explanation

In this section, the steps from the previous section are explained:
determine the maximum amount of the normal reaction force (N) and the friction force (f) and then calculate the hydraulic cylinder diameter and primary design of the wheel shaft will explain. The purpose is to design a schematic of the shaft and the number of its step for mounting other wheel parts on it and assembling of the wheel shaft with ball bearing and then with brake arm. Also, the diameter of the shaft sections (steps) and the proper material for the shaft should be specified with respect to its loading condition. The selected material and diameters must be sufficient to support the applied stresses on the shaft. The designed shaft in this step will be analyzed in ABAQUS in the 3rd step for checking the stresses and deformations of different elements of it.

4.1 Normal Reaction Force (N) and the Friction Force (f)

The purpose of this step is to determine the maximum amount of the normal reaction force (N) and the friction force (f) as shown in Figure 9, which apply to the brake mechanism. Assuming the car has constant acceleration during braking, the following equation is used :

Equation 1 Equation of Motion

$$\int_{x1}^{x2} a\,dx = \int_{v1}^{v2} v\,dv$$

In Equation 1, a is the acceleration,v is the velocity of the car, and x is the car's displacement. As mentioned in the modeling section, the braking distance is 30 meters and the car's speed is 110 km/h. Using Equation 1, the braking acceleration is calculated to be 15.5 m/s². The maximum permissible weight of the car in Figure 11, is 2000 kg. now by using D'Alembert's Principle, the equations of motion are (figure 10):

Equation 2 D'Alembert's Principle

$$\sum F_x = F_F + F_R = \frac{W}{g}a \qquad \sum M_{p_f} = N_R L - W L_f = \frac{W}{g}a h_L$$

Since the brake wheel is installed between the car's rear wheels, N_R is the sum of normal reactions on the car's rear wheels and brake wheels.
Let's have a different look at the problem, assume that the center of mass of the car in Figure 7, is in the middle of the front and rear wheels horizontally and in the middle of

the car height vertically; so, the moment about the front wheel point (Pf in figure 10) due to the car weight and acceleration force are in different directions (-z and z directions in figure 10). The amount of the moments with respect to Figure 11 dimensions and the car acceleration and its weight (2000kg) are as below:

Equation 3 The moments

$$M_W = 2000 \times 9.81 \times \frac{2851}{2} \times 10^{-3} = 27968\ N.m\ \circlearrowright$$

Equation 4 The moments

$$M_a = 2000 \times 15.5 \times \frac{1440}{2} \times 10^{-3} = 22320\ N.m\ \circlearrowleft$$

Equation 5 The moments

$$M_{N_R} = M_w - M_a = 5648\ N.m$$

Equation 6 The maximum achievable normal reaction rear wheels

$$M_{N_R} = N_R\ L\ \longrightarrow N_R = \frac{5648}{2851 \times 10^{-3}} = 1981\ N \rightarrow\ \ for\ both\ of\ the\ rear\ wheels$$

So, at this braking acceleration, the maximum achievable normal reaction force on each of the rear wheel and brake wheel is about 990 N from Eq. 7 (1981N divide by 2).

As mentioned before, the purpose of the first step is to determine the maximum forces that apply to the brake mechanism. Assume that the entire of the 990N apply to brake mechanism and just the brake wheel supports this force. Therefore, a safety factor of about 2 is saved in this section for the normal force (N) that applies to the brake mechanism parts.

The maximum of another force that must be determined is friction force (f). As known static friction force is more than dynamic friction force. The static friction factor of rubber tires on asphalt is 0.8 to 1. So, the maximum amount that can be applied to the brake mechanism equals the normal force N. In this condition, the brake wheel is rolling on the road. If the wheel starts slipping, the friction force will drop at least 20%.
Finally, for simplicity of the calculations, let 990N ≃1000N for **N** and **f** forces in the next analysis step.

4.2 Solve The Equilibrium on The Brake Mechanism

4.2.1 Selection of Hydraulic Cylinder

With having N and f. Then calculating hydraulic cylinder diameter, detail design of brake wheel shaft and selection of the suitable ball bearing for brake wheel.

Eq. 7 shows the equilibrium on Figure 9, so the maximum required hydraulic force is obtained from this equation.

Equation 7 Equilibrium

$$\sum T_R = 0 \rightarrow 508N - 245f - 125h = 0 \ \rightarrow h = \frac{508N-245f}{125}$$

The maximum of h will occur when the friction factor is 0.8 and f is the minimum. Therefore, h max is:

Equation 8 Hydraulic force

$$N = 1000N\ , f = 0.8 \times 1000 = 800N \ \rightarrow h_{max} = 2496N$$

The chosen working pressure of the car's hydraulic pump is about 100 bar because, in the automotive industry and hydraulic system design, a pressure of 100 bar is a common standard used in many systems. This pressure is accepted as a standard value that provides both effective and economical performance.

(Hydraulic & Pneumatic Systems, n.d.)

Therefore, the required piston diameter is:

Equation 9 The diameter of piston needed

$$d = \sqrt{\frac{4h}{p\pi}} = \sqrt{\frac{4*2496}{100\times10^{-1}\times\pi}} = 17.81mm \ \rightarrow let\ d_{piston} = 20\ mm$$

According to Eq.9, the diameter of the hydraulic jack piston is selected as 20 mm.

Now, the Ball bearing will be mounted on the first step of the shaft (from right, figure 8) and then the wheel and bearing will assembly with the arm (figure 3). assume the shaft, at its most pessimistic condition, that the one end of it is fixed, and the forces N and f

apply to it, along its length as a distributed load. In this condition, the bending moment diagram of the shaft in the plane of N and F resultant force is as Figure 8. The magnitude of the resultant force of the N and f is obtained from Eq 10.

Equation 10 Resultant force of the N and f

$$N_{max} = 1000N\ , f_{max} = 1000N\ \rightarrow R = 1000\sqrt{2} \cong 1415N$$

The maximum moment from diagram in Figure 12 is about 290 N.m but due to Stress-concentration factor, the critical point of the shaft is the end of first step that the diameter changes. At this point (30 mm from right, figure 8) the amount of moment is about 270 N.m.

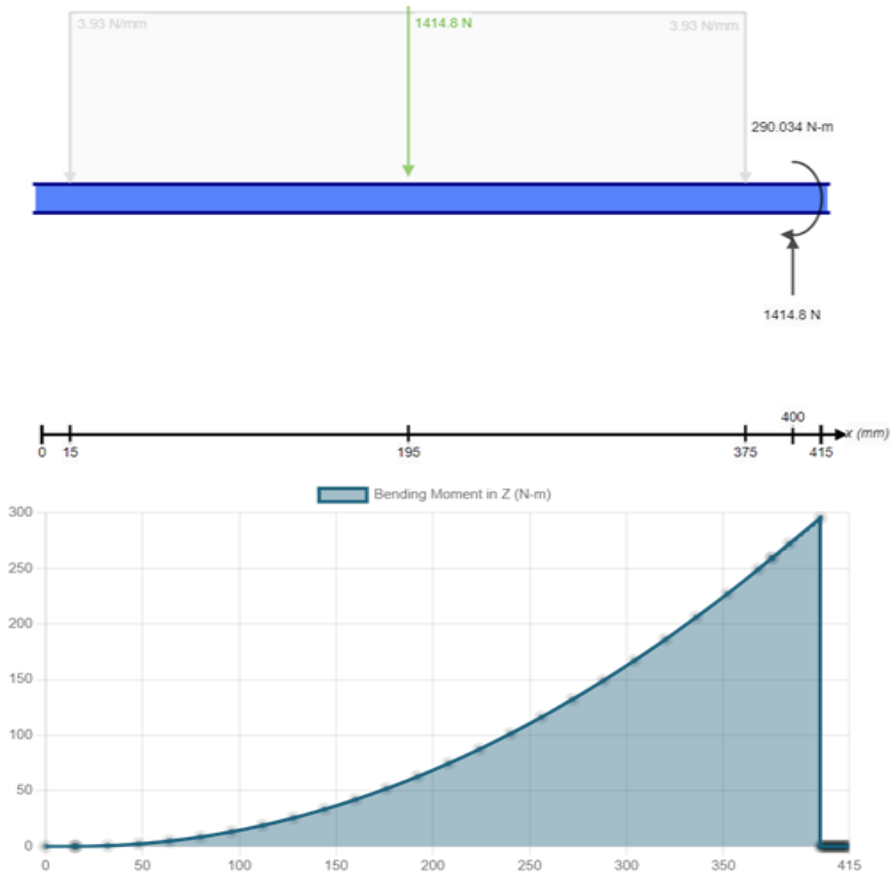

The shaft material is determined in Table 1 and Table 2 indicates the value and definition of the Eq.11 to Eq.14.

Table 1 Parts material properties according to DIN EN 10083 and 10025((Deutsches Institut für Normung, 2006; Deutsches Institut für Normung, 1990).

Parts	**material**	**Yield strength (MPa)**	**Ultimate strength (MPa)**
Arm	1.1221(+QT)	Min. 520	800-950
Wheel shaft	1.7225	Min. 750	1000-1200
Wheel ring	S235jr	Min. 235	380-510
Wheel rubber	Styrene rubber (SBR)	-	-

Table 2 The value and parameters of Eq.11 to Eq.14 (Sprinter, 2022)

Parameter	Value	Unit	Definition
FS	1.35	-	safety factor for fatigue
Kf	1.935	-	Fatigue stress-concentration factor in bending
Kfs	1.475	-	Fatigue stress-concentration factor in torsion
Mm	0	N.m	Moment produces mean stress (σ_m)
Ma	270	N.m	Moment produces alternating stress (σ_a)
Tm	0	N.m	torque produces mean stress (τ_m)
Ta	0	N.m	torque produces alternating stress (τ_a)
Su	1000	Mpa	Material ultimate strength
Sy	750	Mpa	Material yield strength
Se	267.8	Mpa	Modified fatigue endurance limit
Ka	0.878	-	Surface factor of ground finishing
Kb	0.862	-	Size factor
Kc	1	-	Loading factor (bending)
Kd	1	-	Temperature factor
Ke	0.702	-	Reliability factor of 99.99%

4.2.2 Selection of Shaft Diameter

For calculations of the proper shaft diameter considering fatigue and unlimited life for the shaft, Westinghouse code is used that is a combination of MSS, Soderberg and Treska theories. Eq.11 shows the Westinghouse code relation.

Equation 11 Westinghouse code relation

$$d = \sqrt[3]{\frac{32FS}{\pi}\sqrt{k_f^2\left(\frac{M_m}{S_y}+\frac{M_a}{S_e}\right)^2 + k_{fs}^2\left(\frac{T_m}{S_y}+\frac{T_a}{S_e}\right)^2}}$$

$$S_e' = 0.504 S_u$$

$$S_e = k_a k_b k_c k_d k_e k_f \, S_e'$$

Substituting the values of table 2 into Eq. 11 results $\boldsymbol{d = 30\ mm}$ for the critical step of shaft that ball bearing mounts on this step. The other points of the shaft have lower bending moment and larger diameter; so, the stresses in that points are lower than the critical point which is at the first and smallest step of the shaft. therefore, no need to calculate the diameter of the shaft in the other steps and no fatigue and failure will occur on the other points of the shaft.

4.2.3 Selection of Bearing for The Brake Wheel

After determining the diameter of the shaft in the bearing seat, the last section of this step is selection of the proper bearing for the brake wheel (figure 4). First the bearing type must be selected. Since the moment applies to the bearing, according to the bearings manufacturer catalogues, match pair angular contact ball bearing or double row angular contact ball bearing must be selected. Figure 13 shows the double row angular contact ball bearing used in car front wheels.

Figure 13 Double row angular contact ball bearing in cars front wheel (KOYO,2023)

With respect to shaft diameter in the bearing seat, the ball bearing inner diameter is 30 mm. The selected brand for choosing angular contact ball bearings is KOYO. Now by referring to the KOYO catalog proper bearing will be selected. The selected bearing is 5206 2RS. The bearing has a rubber seal on both sides. These contact seals prevent the penetration of contamination into the bearing. The bearing life is calculated with respect to bearing loading conditions. Figure 14 shows the bearing cross-section

dimensions and specification table. The last row in Figure 14 shows the selected bearing specification (d=30 mm).

Figure 14 KOYO double row angular contact ball bearing specification (KOYO, 2023)

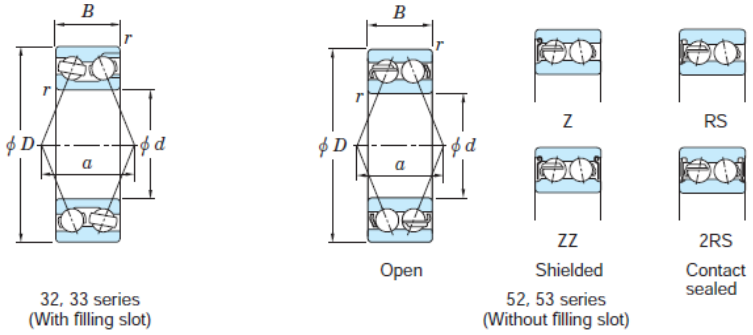

Boundary dimensions (mm)				Basic load ratings (kN) Open		Shielded/sealed		Fatigue load limits (kN) C_u		Limiting speeds (min⁻¹) Grease lub.		Oil lub.	Bearing No.			Load center spread (mm)	Mounting dimensions 1) (mm)				(Refer.)
d	D	B	r min.	C_r	C_{0r}	C_r	C_{0r}	(Open)	(Shielded/sealed)	(Open Z, ZZ)	(RS, 2RS)	(Open Z)	Open	Shielded	Sealed	Open a	d_a min.	d_a max.	D_a max.	r_a max.	Mass (kg)
10	30	14.3	0.6	9.15	5.35	—	—	0.280	—	15 000	—	20 000	3200	—	—	19.5	14.5	—	25.5	0.6	0.052
12	32	15.9	0.6	12.1	7.15	—	—	0.370	—	14 000	—	18 000	3201	—	—	21.7	16.5	—	27.5	0.6	0.063
15	35	15.9	0.6	12.1	7.45	—	—	0.390	—	12 000	—	16 000	3202	—	—	23.6	19.5	—	30.5	0.6	0.072
	42	19	1	19.0	11.9	—	—	0.610	—	10 000	—	14 000	3302	—	—	27.6	20.5	—	36.5	1	0.132
17	40	17.5	0.6	17.2	10.8	—	—	0.560	—	11 000	—	14 000	3203	—	—	26.6	21.5	—	35.5	0.6	0.100
	40	17.5	0.6	16.5	8.15	15.9	8.35	0.420	0.430	11 000	11 000	14 000	5203	5203 ZZ	5203 2RS	20.0	21.5	23.5	35.5	0.6	0.091
	47	22.2	1	23.0	17.1	—	—	0.760	—	9 400	—	13 000	3303	—	—	31.0	22.5	—	41.5	1	0.192
20	47	20.6	1	21.5	15.0	—	—	0.770	—	9 000	—	12 000	3204	—	—	31.5	25.5	—	41.5	1	0.170
	47	20.6	1	24.6	12.5	20.0	10.8	0.640	0.560	8 800	8 800	12 000	5204	5204 ZZ	5204 2RS	23.5	25.5	26.6	41.5	1	0.158
	52	22.2	1.1	26.0	18.4	—	—	0.950	—	8 200	—	11 000	3304	—	—	33.8	27	—	45	1	0.230
	52	22.2	1.1	30.9	15.0	24.7	12.8	0.780	0.660	8 300	8 300	11 000	5304	5304 ZZ	5304 2RS	25.9	27	28.3	45	1	0.230
25	52	20.6	1	23.7	18.2	—	—	0.940	—	7 800	—	10 000	3205	—	—	34.4	30.5	—	46.5	1	0.190
	52	20.6	1	26.7	14.8	23.6	13.8	0.760	0.710	7 700	7 700	10 000	5205	5205 ZZ	5205 2RS	26.1	30.5	32.3	46.5	1	0.190
	62	25.4	1.1	36.2	26.5	—	—	1.35	—	6 800	—	9 100	3305	—	—	40.5	32	—	55	1	0.369
	62	25.4	1.1	40.9	20.8	34.3	18.5	1.05	0.960	6 900	6 900	9 200	5305	5305 ZZ	5305 2RS	31.1	32	33.4	55	1	0.340
30	62	23.8	1	34.1	27.0	—	—	1.40	—	6 500	—	8 700	3206	—	—	40.7	35.5	—	56.5	1	0.320
	62	23.8	1	37.2	21.3	31.7	18.3	1.10	0.950	6 400	6 400	8 600	5206	5206 ZZ	5206 2RS	30.8	35.5	38.6	56.5	1	0.290
	72	30.2	1.1	47.7	36.1	—	—	1.85	—	5 800	—	7 800	3306	—	—	47.2	37	—	65	1	0.585
	72	30.2	1.1	51.2	28.5	42.9	25.2	1.45	1.30	5 800	5 800	7 700	5306	5306 ZZ	5306 2RS	36.2	37	41.3	65	1	0.510

The bearing basic rating life based on running distance is calculated with Equation 12: (ISO 281:1990)

Equation 12 Bearing basic rating life

$$L_{10s}(km) = \pi D(mm) L_{10}(10^6 rev)$$

$$L_{10} = \left(\frac{C}{P}\right)^p$$

$$L_{nm} = a_1 a_{ISO} L_{10}$$

L_{10s} is The bearing lifespan is based on the distance traveled ,L_{10} is the basic bearing life in million revolutions,D is wheel diameter in mm, C is the basic dynamic load rating of bearing in kN, P is the dynamic equivalent load in kN, and p=3 for ball bearings. L_{nm} is modified rating life in million revolutions with respect to reliability factor a_1 and ISO factor a_{ISO}.

Let reliability 99%, according to KOYO catalog, $a_1 = 0.25$.

a_{ISO} depends on three factors, fatigue load limit C_u, viscosity ratio k, and contamination factor e_c.so, for keeping on the calculation, the dynamic equivalent load P, must be determined. The catalog presents Eq.13 for the calculation of dynamic equivalent force and Eq.14 for static equivalent force.

Equation 13 Dynamic equivalent force

$$P_r = XF_r + YF_a$$

Equation 14 Static equivalent force

$$P_{0r} = X_0F_r + Y_0F_a$$

Figure 15 The KOYO double row angular contact ball bearing factors (KOYO, 2023).

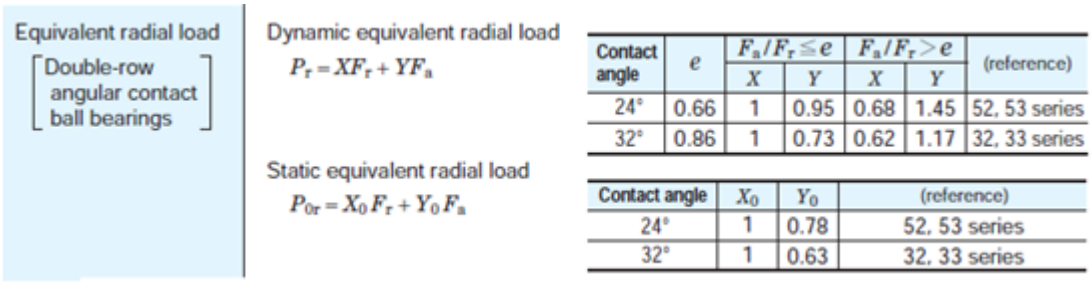

Equivalent radial load

Double-row angular contact ball bearings

Dynamic equivalent radial load

$P_r = XF_r + YF_a$

Static equivalent radial load

$P_{0r} = X_0F_r + Y_0F_a$

Contact angle	e	$F_a/F_r \leq e$		$F_a/F_r > e$		(reference)
		X	Y	X	Y	
24°	0.66	1	0.95	0.68	1.45	52, 53 series
32°	0.86	1	0.73	0.62	1.17	32, 33 series

Contact angle	X_0	Y_0	(reference)
24°	1	0.78	52, 53 series
32°	1	0.63	32, 33 series

As mentioned above (Eq. 11 and figure 9), the force R applies to the shaft and the bearing must support it. For calculations of F_r and F_a, according to the catalogue (Figure 16), there are following equations:

$$F_{rA} = \frac{b}{c} R \qquad (21)$$

$$F_{rB} = \frac{a}{c} R \qquad (22)$$

$$F_{aA,B} = \frac{F_{rA,B}}{2Y} \qquad (23)$$

Figure 16 Picture from KOYO catalogue (KOYO, 2023)

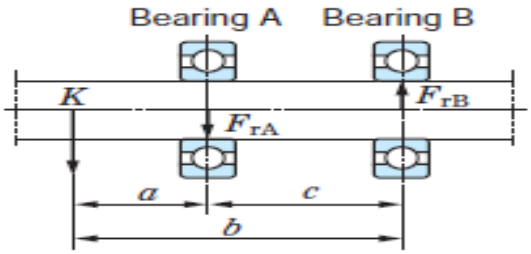

K in Figure 16 is equivalent to R in Eq. 21 and Eq. 22. A and B in figure 16 and Eq. 21 and Eq. 22 are equivalent to the rows of the selected double-row angular contact ball bearing. The values of a, b, and c in figure 16 are determined in figures 4, 8 and 12. C in figure 16 is determined in figure 14 as a in column 'load center speared'. A 200N force is assumed as preload for the bearing and is added to the axial load of the bearing F_a. By substituting the values in the above equations, the results **of dynamic equivalent force** are as below:

$$F_r = 10.25kN \uparrow$$

$$F_{aA} - F_{aB} + 0.2 = 1kN \rightarrow$$

$$P = 1 \times 10.25 + 0.95 \times 1 = 11.2kN \qquad (24)$$

The bearing speed is required to be determined. The speed of movement could vary, but the calculations were started with a speed of 110 km/h, which is the highway speed. As continue, based on the range specified in the bearing manufacturer's catalog, it will be determined up to what speed range the bearing can handle. This

speed is equal to about 1833 m/min. The brake wheel diameter is 180mm. So, the bearing speed is calculated from Eq. 15:

Equation 15 Bearing speed

$$n(rpm) = \frac{V\left(\frac{m}{\min}\right)}{\pi D(mm)} \cong 3200rpm \text{ (max)}$$

Equation 16 Outside and bore diameter of the bearing

$$D_{pw} = \frac{D+d}{2} = 46mm$$

D and d in Eq. 16 are the outside and bore diameter of the bearing, respectively (figure 14).

Now a_{ISO} can be calculated according to the catalogue as below:

With D_{pw} and n from the diagram in the catalog, $\nu_1 = 12\frac{mm^2}{s}$.

viscosity ratio, k, is determined by Eq. 17:

Equation 17 Viscosity ratio

$$k = \frac{\nu}{\nu_1}$$

$$e_c = 0.6 \rightarrow standard\ cleanlines, KOYO\ catalogue$$

Figure 17 Standard cleanlines,KOYO catalogue(KOYO, 2023)

Contamination level	e_c	
	$D_{pw} < 100$ mm	$D_{pw} \leqq 100$ mm
Extremely high cleanliness: The size of the particles is approximately equal to the thickness of the lubricant oil film, this is found in laboratory-level environments.	1	1
High cleanliness: The oil has been filtered by an extremely fine filter, this is found with standard grease-packed bearings and sealed bearings.	0.8 to 0.6	0.9 to 0.8
Standard cleanliness: The oil has been filtered by a fine filter, this is found with standard grease-packed bearings and shielded bearings.	0.6 to 0.5	0.8 to 0.6
Minimal contamination: The lubricant is slightly contaminated.	0.5 to 0.3	0.6 to 0.4
Normal contamination: This is found when no seal is used and a coarse filter is used in an environment in which wear debris and particles from the surrounding area penetrate into the lubricant.	0.3 to 0.1	0.4 to 0.2
High contamination: This is found when the surrounding environment is considerably contaminated and the bearing sealing is insufficient.	0.1 to 0	0.1 to 0
Extremely high contamination	0	0

$C_u = 0.95kN \rightarrow figure\ 14$

$\frac{e\ C_u}{P} = 0.05$

viscosity ratio from KOYO catalogue k=4, then from the radial ball bearing diagram in the catalog:

$a_{ISO} = 3.$

Because of the brake wheel's impact on the ground at the instance of braking, a load coefficient for load should be considered. Let $f_w = 2$ according to the KOYO catalog for severe impact. Finally, by substituting the values of f_w, a_1, a_{ISO} and Eq. 16 into Eq. 17, the bearing life in terms of running distance is calculated from Eq. 18 with a reliability of 99%.

Equation 18 Bearing life

$$L_{10s} = \pi \times 180 \times 0.25 \times 3 \times \left(\frac{31.7}{11.2\times2}\right)^2 = 850\ km$$

Since the brake does not work permanently and just at braking time the brake wheel rotates and the load applies to the bearing and the braking distance is maximum 30 meters, so the bearing life in Eq. 18 is sufficient.

The static equivalent load of the bearing from Eq.14 and figure 15 is:

Equation 19 Static equivalent load

$$P = 1 \times 10.25 + 0.78 \times 1 = 11kN$$

And static safety factor with respect to basic static load rating is:

Equation 20 Static safety factor

$$f_s = \frac{C_0}{P_0} = \frac{18.3}{11} = 1.66$$

Based on the calculations and analysis performed, the selected bearing (KOYO 5206 2RS) is deemed suitable for use in the brake wheel of the vehicle. The reasons for this conclusion are as follows:

1. **Bearing Life:** The calculated bearing life based on running distance (850 km) is significantly higher than the actual operational needs, as the bearing is only loaded during braking, which is up to a maximum distance of 30- 60 meters. Therefore, the bearing will perform adequately throughout its expected lifespan.

2. **Dynamic Loading:** The calculated dynamic equivalent load (11.2 kN) is within the permissible load limits of the bearing as per the provided specifications and standards.the bearing is capable of handling the expected loads.

3. **Bearing Speed:** The bearing speed at maximum operational conditions (3200 rpm) is within the allowable speed range of the selected bearing. Even if this speed were to double, the bearing would still be able to handle it according to the catalog specifications.Thus, the bearing will operate efficiently without any issues related to speed.

4. **Static Safety Factor:** The calculated static safety factor (1.66) exceeds the minimum required safety factor for static loads, indicating that the bearing is also suitable for static load conditions.

Considering all the factors and calculations, the KOYO 5206 2RS bearing is suitable for the brake wheel application due to its compatibility with the required lifespan, load capacity, operational speed, and static safety factor. Therefore, this bearing can be confidently used in the system.

4.3 Mechanism Designed in SOLIDWORKS

In this step, the brake mechanism is designed in SOLIDWORKS (SolidWorks Dassault Systèmes, 2023), and shows the exported model into ABAQUS. In the assembly module instances are created from the brake parts and an assembly is created. As illustrated in Figure 18, for having a better and regular meshes on the parts, sufficient partitions also were created.
(Abaqus Dassault Systèmes, 2022)

Figure 18 The brake mechanism 3D-model in ABAQUS software

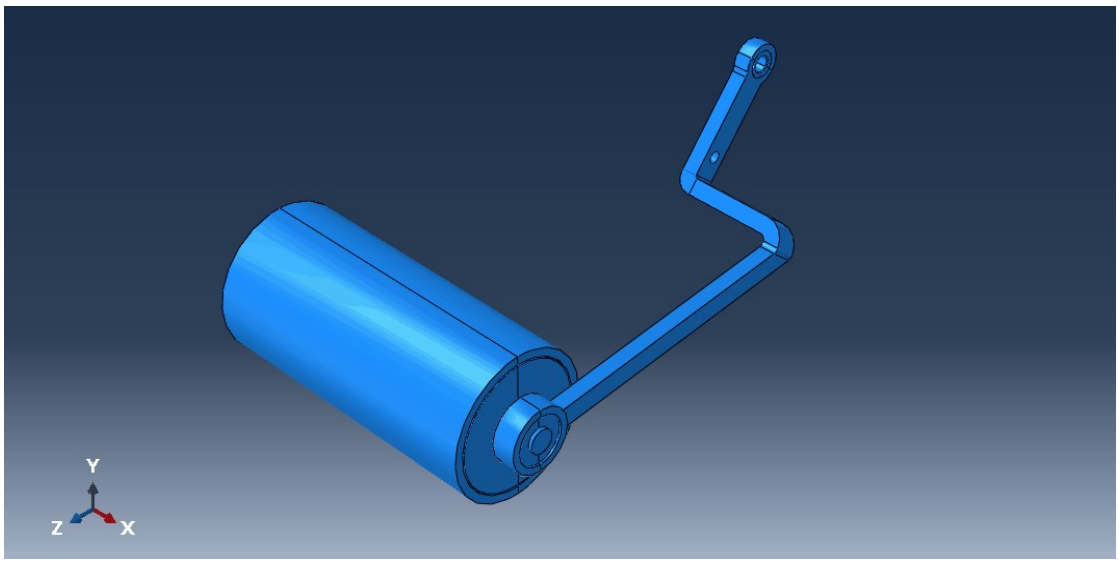

The material of the arm, shaft, ring, and bearing is defined as steel. Young's modulus and Poisson's ratio for steel elastic property is 200 GPa and 0.3 respectively. The material of the wheel is defined as styrene rubber- a common rubber material of car wheels- and is defined as a hyperelastic material with specifications shown in Figure 18.

According to the modeling section and the explanation, a static general step was created for the analysis. Then suitable interaction between parts is defined. The boundary condition in the initial step was defined. Since the brake is fixed relative to the car during braking, the upper hole of the arm connects to the car chassis via a

revolute joint, allowing the system to rotate only around the main pin where it is attached to the chassis, while being fixed in all other movements and rotations.

Figure 19 Wheel rubber specification

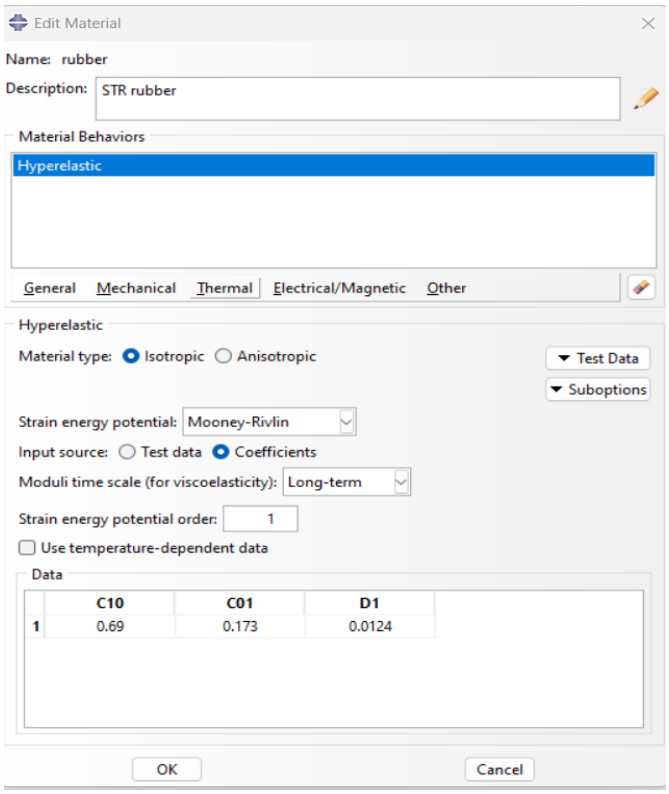

The hydraulic force applied to the arm perpendicularly, Normal force (N) along Y direction and the friction force (f) along -Z direction. N and f distributed along the wheel length (figure 20).

Figure 20 shows the boundary condition and 3-loads defined on the mechanism: hydraulic force, normal reaction, and friction force.

Figure 20 Loading on the mechanism

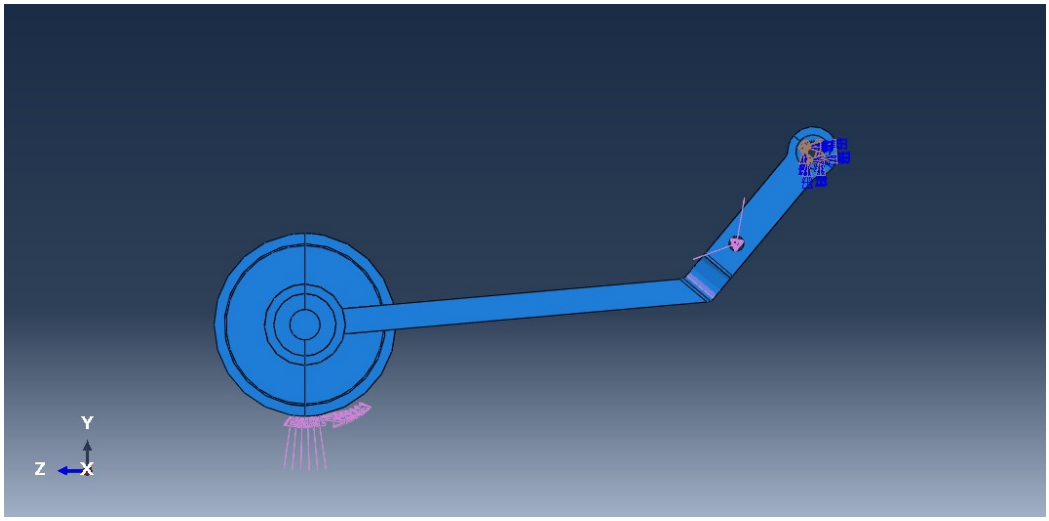

Figure 21 shows the meshed mechanism. The parts seeded and meshed separately and proportional to its dimensions. For example, the mesh size in the wheel is larger than the shaft. Figure 21 and 22 and 23 show detail of generated mesh.

Figure 21 Meshed mechanism in ABAQUS

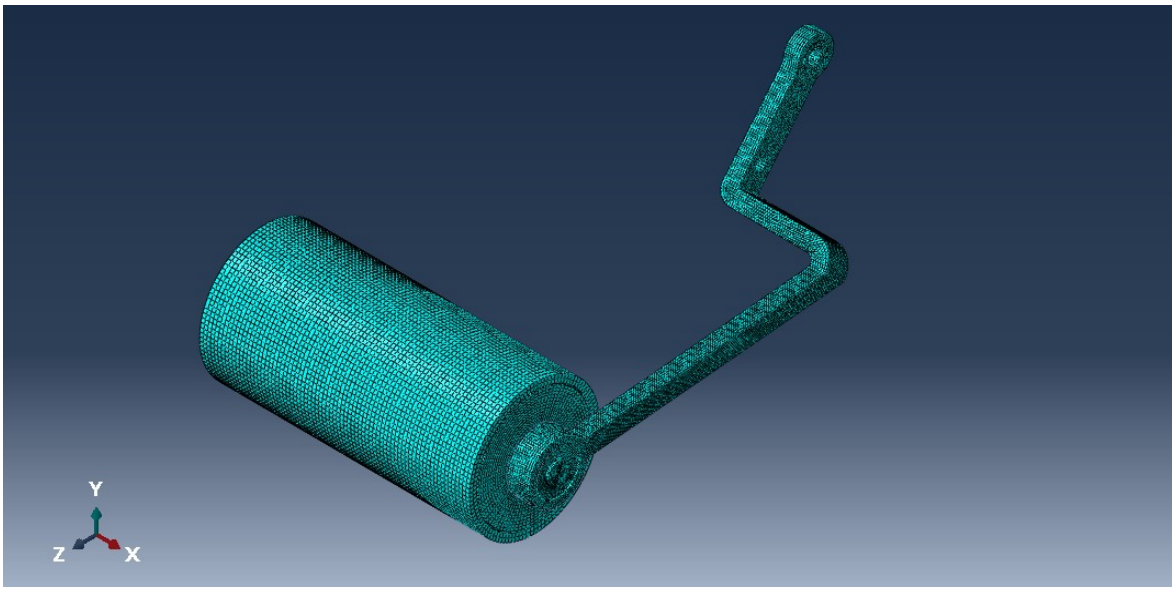

Figure 22 Generated mesh on the shaft

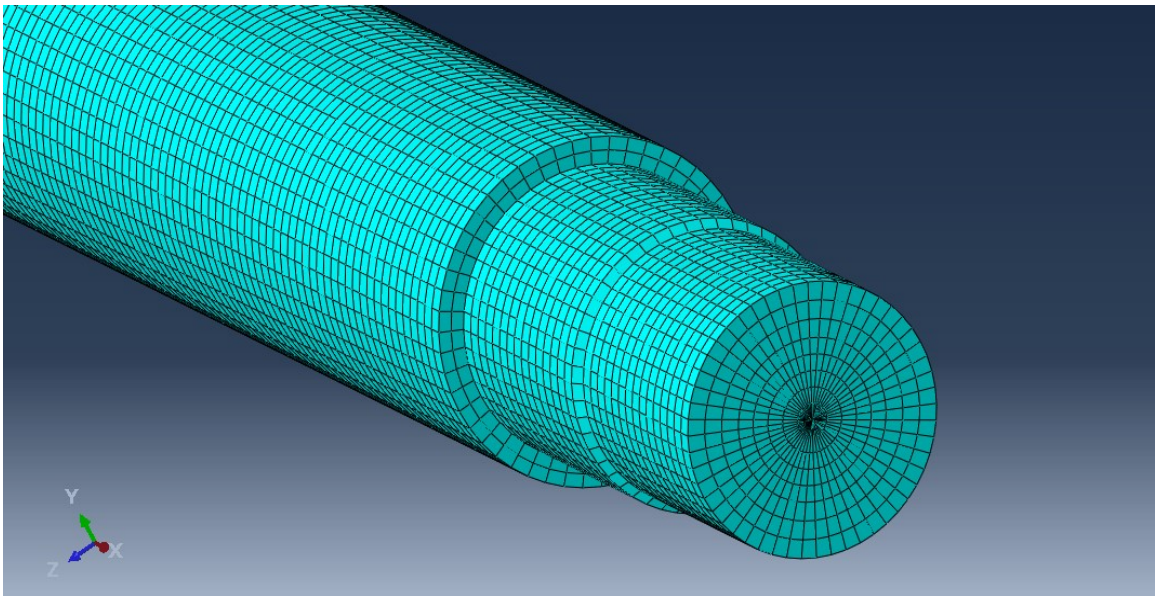

Figure 23 Generated mesh on the arm

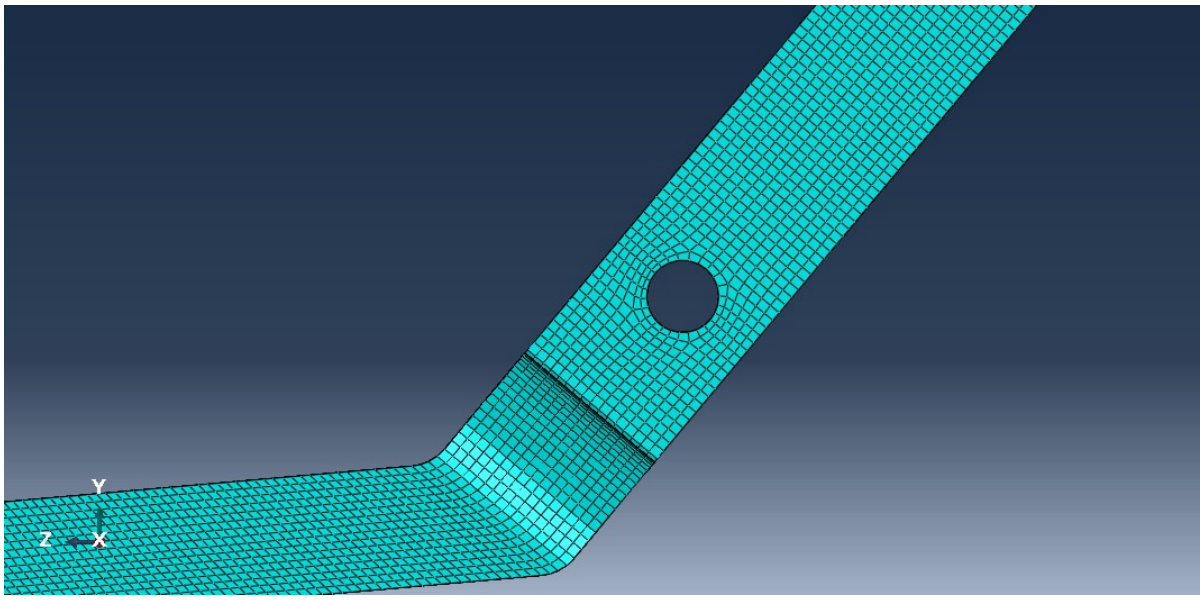

Figure 24 and 25 shows the element shape and element size of the instances settings in ABAQUS mesh module.

Figure 24 Mesh element shape

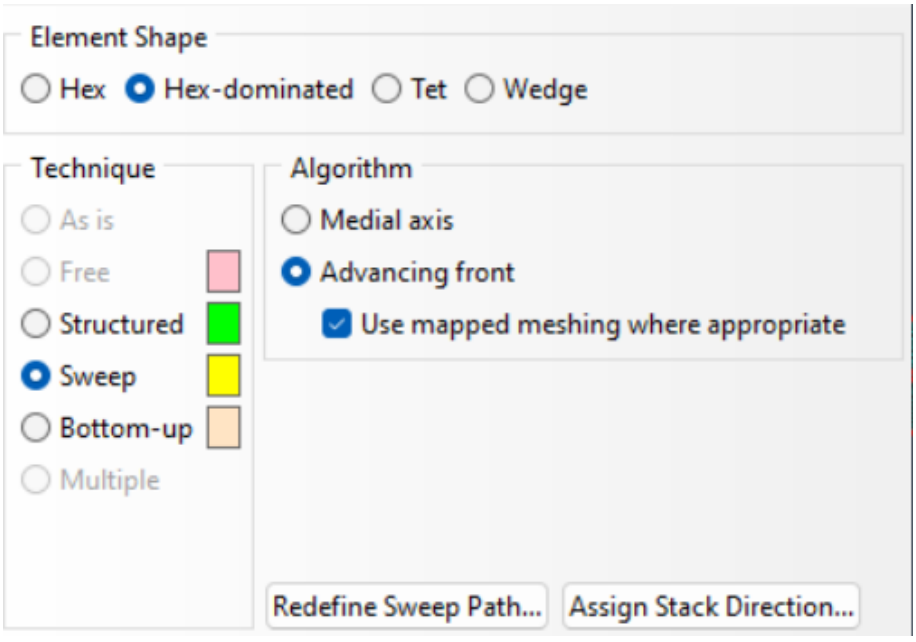

Figure 25 Mesh element type

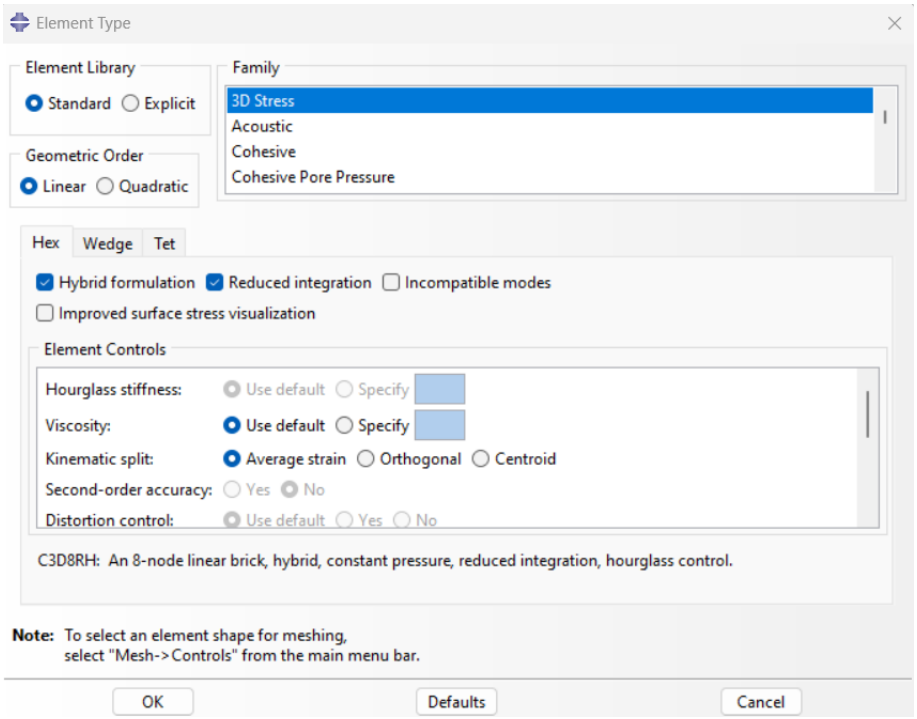

5 Results

The results of this analysis are presented:
Finite element simulation in the brake mechanism are presented in contours as below Figures. In these Figures, S is the stress component at integration points in MPa and U is the magnitude of the spatial displacement at nodes in millimeter.

5.1 Maximum Stress value in The Brake Mechanism

Figure 26 shows the Von Mises stress in the brake mechanism. The maximum stress value is 356 Mpa, which occurs in the brake arm and at the point that is illustrated in Figure 26 as the maximum node. The value of the maximum stress is sufficiently less than the yield strength of the selected material in table1.

Figure 26 Von Mises stress contour of the brake mechanism

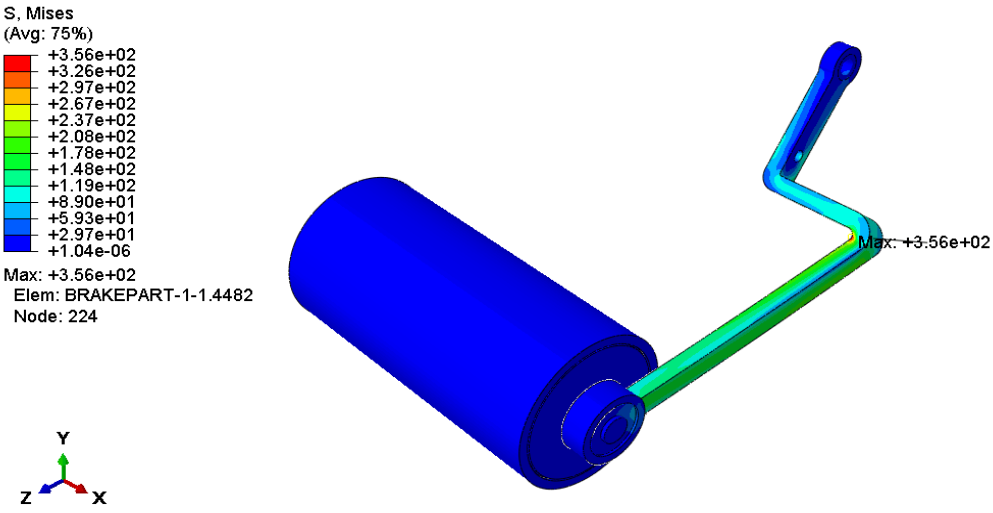

5.2 Results on Arm Strength

The selected material, as indicated in Table 1, is utilized for the arm. Figure 26 provides a closer view of the maximum stress location on the arm. As mentioned in previous paragraphs, a static safety factor of approximately 1.5 has been considered

to prevent arm failure due to the determined forces. Additionally, in the first step of Section 4 (Analysis Explanation), a safety factor for the forces
N and f was also incorporated. These safety factors (1.5 × 2 = 3), along with the assumption of maximum values for f, N, the friction coefficient, and other relevant parameters, compensate for the dynamic effects of the forces N and f.

5.3 Fatigue Analysis at The Maximum Stress Point

A fatigue analysis for the arm at the maximum stress point can be performed. Since the maximum stress is less than the yield strength of the arm material, low-cycle fatigue due to the yielding of critical points does not occur. Therefore, the fatigue life in terms of the number of cycles can be calculated.

When the brake is applied and the wheel brake contacts the ground, the stress in the arm starts to increase from 0 to the maximum calculated value, and then it decreases to 0 once the car comes to a stop.

The model's results demonstrate that the selected material and design are capable of withstanding the applied forces with sufficient safety margins. The consideration of static and dynamic safety factors ensures the arm's integrity under operating conditions. Furthermore, the fatigue analysis confirms that the arm can endure the cyclic loading without experiencing low-cycle fatigue, thus ensuring its durability and reliability throughout its service life. Suresh (2001)

The following relations are used to calculate the fatigue life and stress cycles:

$$\sigma_a' = \sigma_m' = \frac{\sigma_{max} \pm \sigma_{min}}{2} = \frac{356 \pm 0}{2} = 178\ MPa$$

$$S_e' = 0.504 \times 800 = 403.2\ MPa$$

$$k_a = 0.76 \rightarrow machined\ surface\ finish$$

$$k_b = 0.893 \rightarrow A\ 20 \times 35\ rectangular$$

$$k_c = 1$$

$$k_d = 1$$

$$k_e(99.99\%) = 0.702$$

$$S_e = 192\ MPa$$

$$\sigma'_a < S_e \rightarrow unlimited\ life$$

So, the arm has enough fatigue endurance limit and sufficient cycle of life. Also the maximum required number of opening and closing of the brake can be calculated. If the driver every 20 km puts the brake on and the car moving distance be 50000km in every year, after 10 years, the number of the brake arm loading cycle (moving up and down of the brake arm) is:

$$N_{req.} = \frac{50{,}000 \times 10}{20} = 25 \times 10^3\ cycles \rightarrow 10^3 < N_{req} < 10^6$$

According to the wöhler curve of fatigue life, the number of required cycles N_{req}, is in the range of high cycle finite life. Therefore, the arm strength and fatigue life are sufficient.

Figure 27 Von Mises stress contour of the brake mechanism

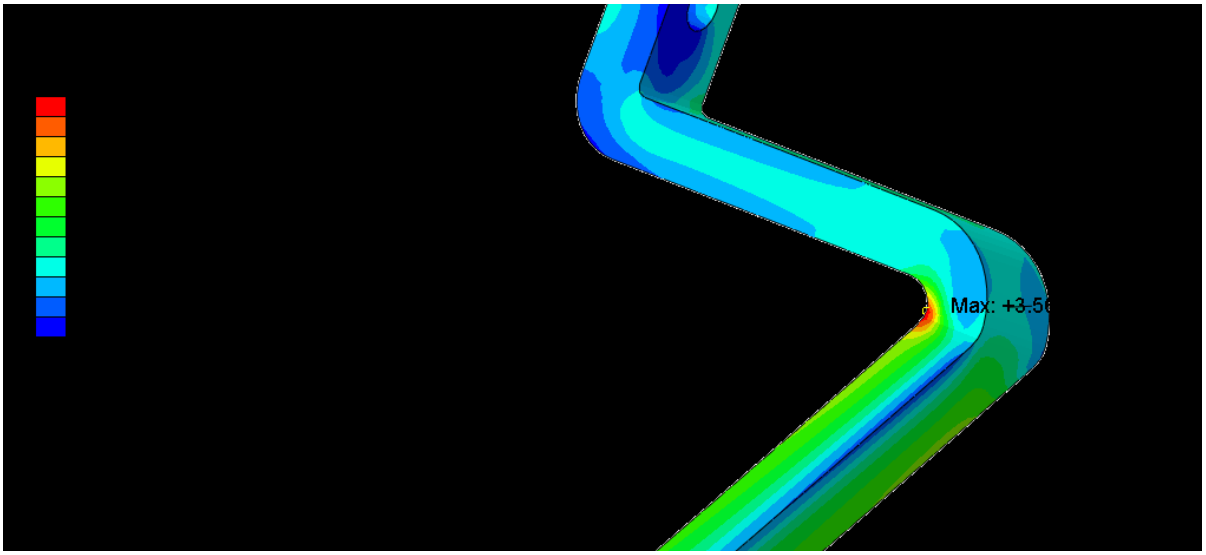

Figure 28 shows the unformed and deformed view of the arm. The maximum of U is 11.6 mm. also the location of the node is illustrated.

Figure 28 Von Mises stress contour of the brake mechanism

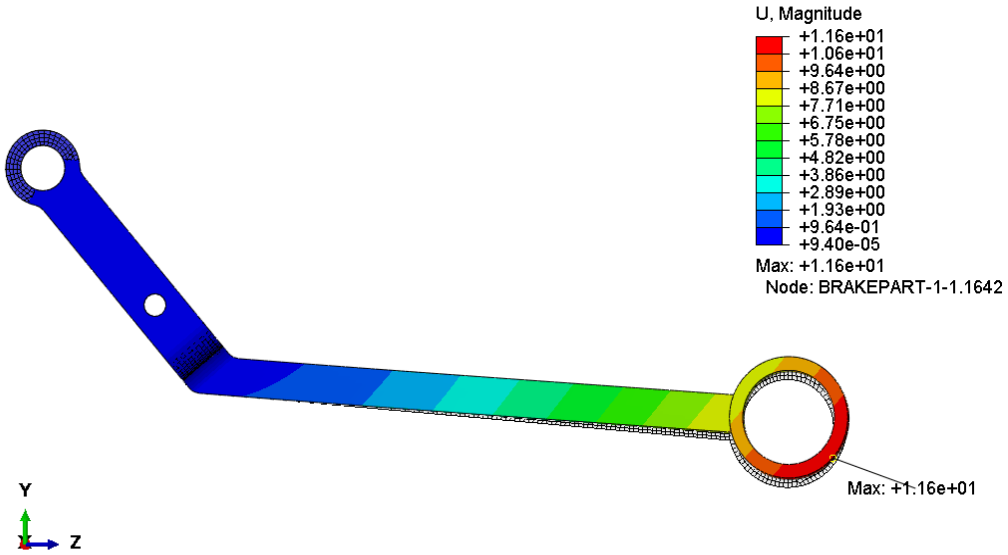

5.4 Deformed Shape of The Brake Mechanism

Figure 29 and 30 shows the unformed and deformed shape of the brake mechanism from different views. The maximum displacement occurs at the end of the wheel and is about 25 mm.

Figure 29 Displacement of the brake mechanism, ISO metric view

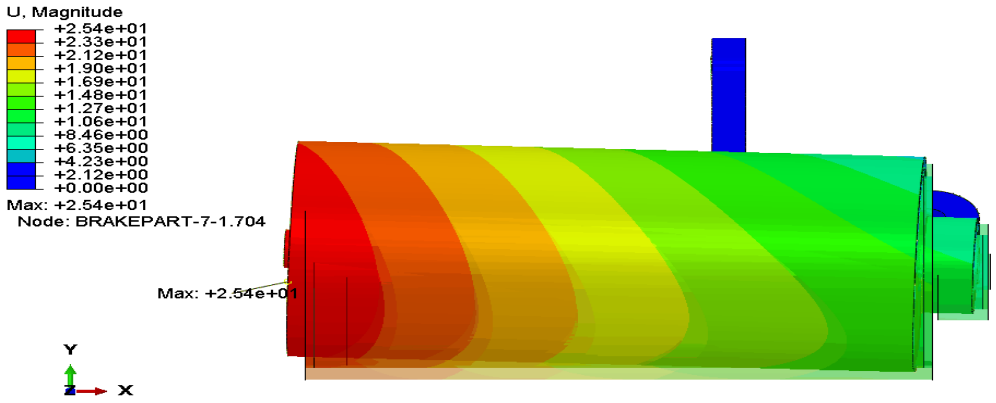

Figure 30 Displacement of the brake mechanism

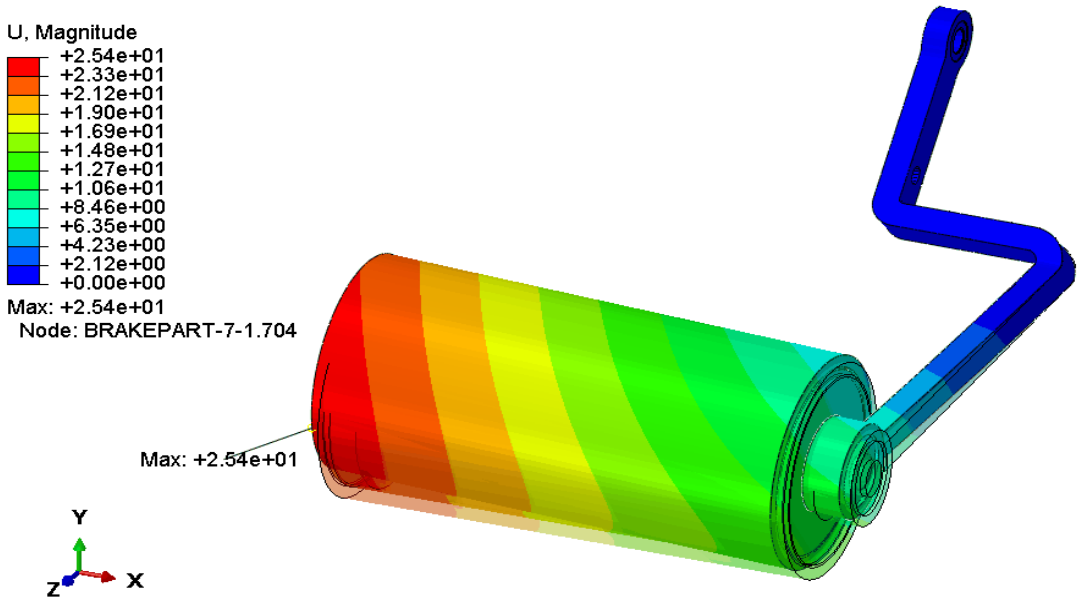

5.5 Stress in The Brake Shaft

Figure 31 shows the stress in the brake shaft. The maximum value is about 96 MPa and its location is at the first step of the shaft in the smallest diameter. With respect to table 2, the fatigue safety factor is obtained again:

$$(FS)_f = \frac{S_e}{k_f \times \sigma'_a} = \frac{267.8}{1.935 \times 96} = 1.44$$

So, the safety factor is near that in table 2 and the calculation in both method is reliable and safe. Also, the material strength of the shaft is good enough.

Figure 31 The stress distribution in the brake shaft

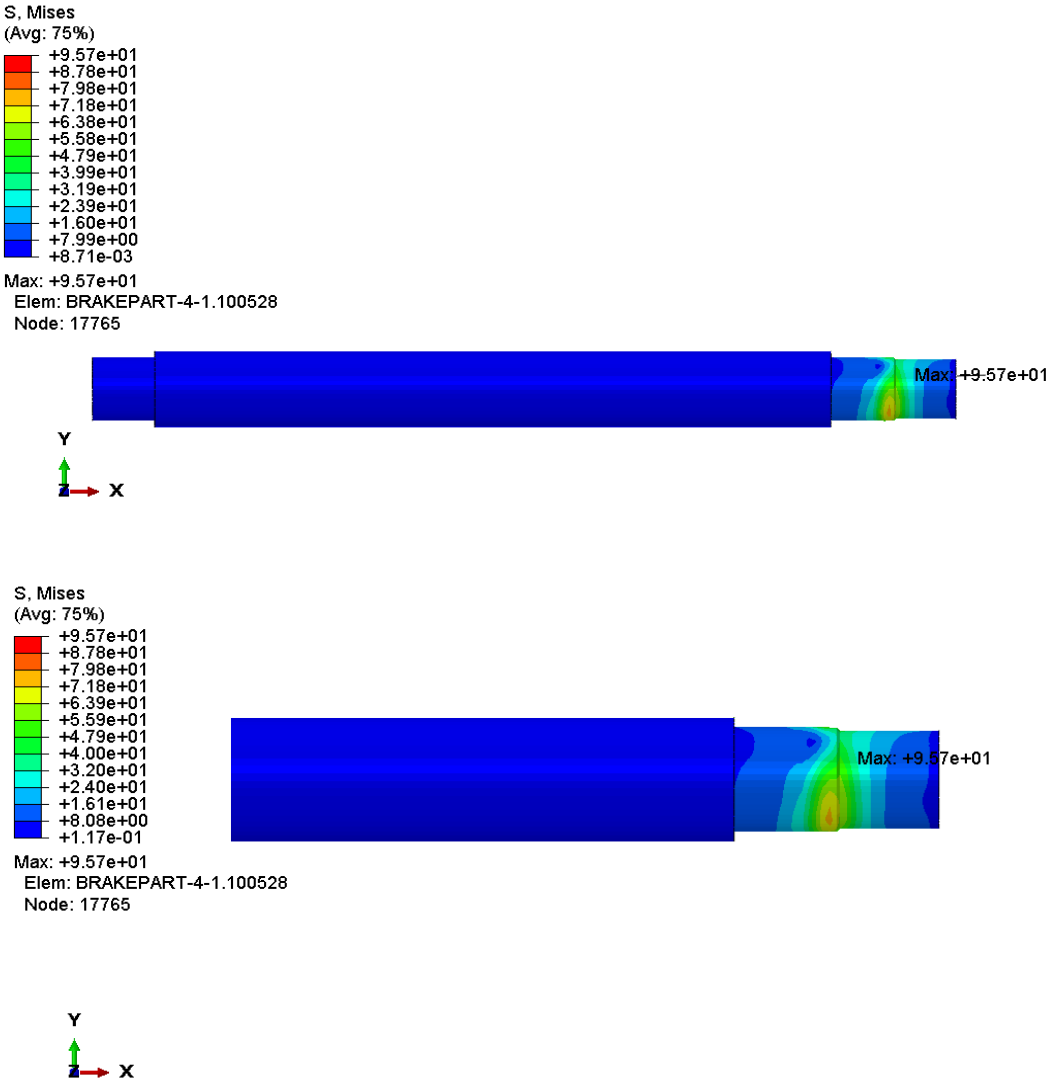

5.6 Stress Distribution within The Wheel Ring

Figure 32 illustrates the stress distribution within the wheel ring under specified loading conditions. The analysis reveals that the maximum stress, occurring in the red region, is approximately 29 MPa. The material used for the ring, S235JR, demonstrates sufficient strength to withstand this stress level, ensuring the ring's structural integrity.

To further optimize the manufacturing process, a thinner plate for the ring could be considered. However, the current thickness offers several advantages, particularly in terms of ease and efficiency in welding, rolling, forming, and assembling processes. Additionally, maintaining this thickness minimizes deformation, thereby enhancing the overall durability and performance of the ring.

the current design, material selection, and manufacturing considerations collectively contribute to the effective performance of the wheel ring under the applied loads. This approach not only ensures structural reliability but also promotes manufacturing efficiency, balancing the mechanical and practical requirements of the wheel ring's application.

Figure 32 The stress distribution in the brake wheel ring

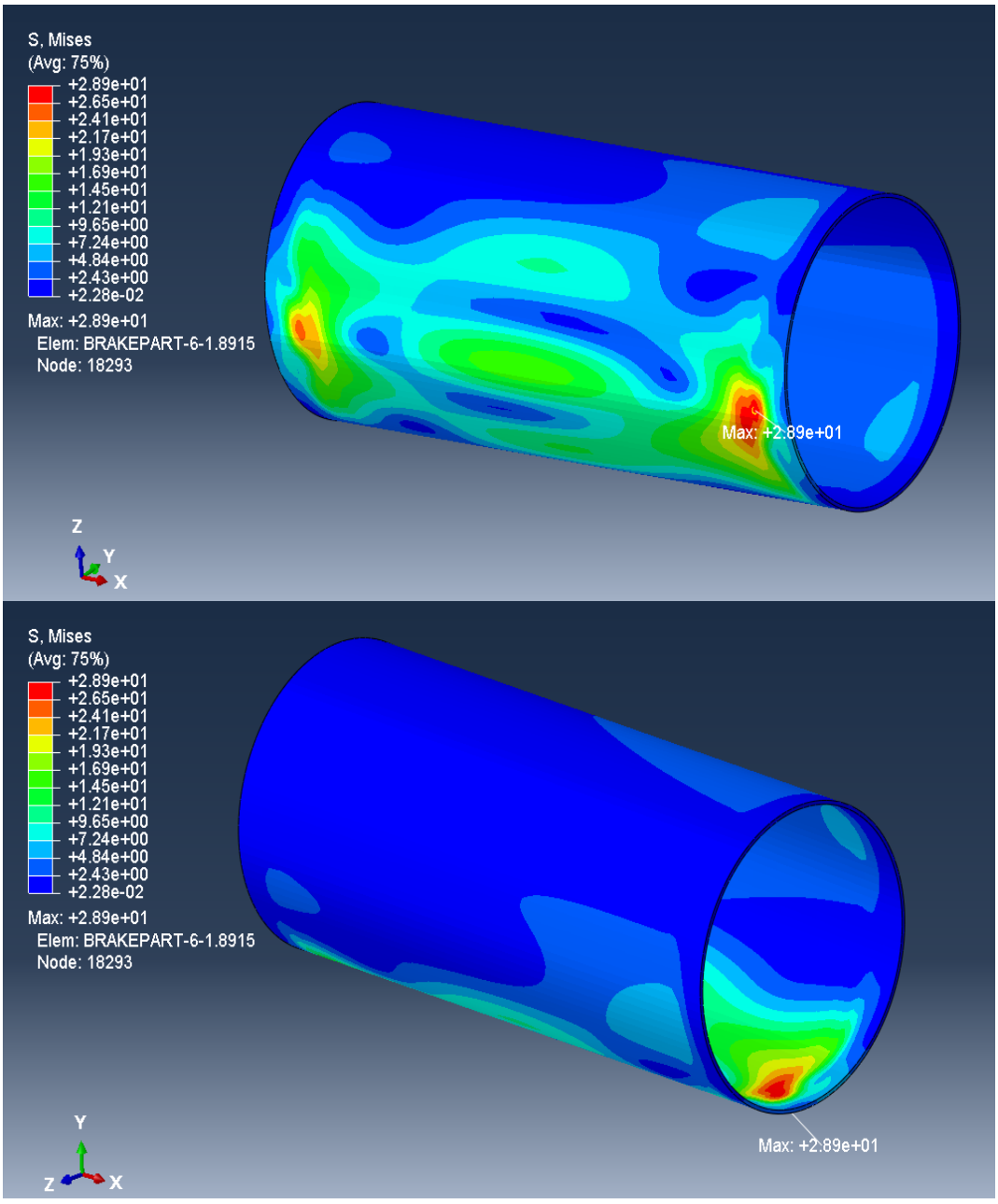

6 Conclusions

In this thesis, the need for better braking systems was identified because vehicles are getting faster and more powerful. The main goal was to create and test a new braking mechanism based on my patented idea.

Throughout the work, each objective was carefully addressed. A detailed 3D model of the braking mechanism was created using SolidWorks, which served as the basis for further analysis. The stress and deformation of the mechanism were thoroughly analyzed using ABAQUS, showing important insights into how forces affect the brake during operation. The analysis showed that the arm experiences the most stress, and the end of the brake wheel has the most displacement, mainly due to bending and twisting of the arm and shaft.

Additionally, the design of each component, except for the helical rotor (which is a braking part), was completed, including material selection.The fatigue analysis showed that the brake arm and brake shaft have a long life under the given conditions. The wheel ring's characteristics were found to be good enough for effective braking.

In conclusion, the research achieved its goals. The design of the mechanism, validated by dynamic analysis and stress evaluation, proves it can be used in real automotive braking systems. However, more research is needed on the helical rotor, as its braking function requires further study.

This work marks a significant step forward in braking technology and provides a foundation for future developments in modern vehicles.

7 References

BMW. (2024). *BMW 7 Series Sedan Technical Data*. Retrieved July 24, 2024, from https://www.bmw-me.com/en/all-models/7-series/sedan/2022/bmw-7-series-sedan-technical-data.html#tab-0

Brembo. (n.d.). *Braking Performance in Formula 1.* Motosport Guide. Retrieved from https://www.motosport-guide.com

Deutsches Institut für Normung. (1990). *Hot rolled products of structural steels – Part 1: General technical delivery conditions (DIN EN 10025-1)*. Berlin: DIN

Dassault Systèmes. (2022). *Abaqus* (Version 2022) [Computer software]. Retrieved from https://www.3ds.com/products-services/simulia/products/abaqus

Dassault Systèmes. (2023). *SolidWorks* (Version 2023) [Computer software]. Retrieved July 24, 2024, from https://www.solidworks.com

Hydraulic & Pneumatic Systems. (n.d.). *Automotive hydraulics*. Retrieved from https://www.hydraulicspneumatics.com

ISO 281:1990. *Rolling bearings — Dynamic load ratings and rating life.* International Organization for Standardization, 1990. Available at: https://www.iso.org/obp/ui/#iso:std:iso:281:ed-2:v1:en

Johnson, M. T. (2018). *Dynamic Analysis of Braking Mechanisms*. Journal of Mechanical Engineering, 45(3), 123-145

KOYO. (2023). *Double row angular contact ball bearing specification*. Retrieved from https://www.koyo.com/double-row-angular-contact-ball-bearing-specification

KOYO. (2023). *Double row angular contact ball bearing in car front wheel*. Retrieved from https://www.koyo.com/double-row-angular-contact-ball-bearing-in-cars-front-wheel

National Highway Traffic Safety Administration (NHTSA). (2023). *Highway rule for typical stopping distances*. Retrieved from https://www.nhtsa.gov/search?q=stopping-distances#gsc.tab=0&gsc.q=stopping-distances&gsc.page=1

Smith, J., & Johnson, A**.** (2023). *Braking acceleration of different types of cars*

Suresh, S. (2001). Fatigue of structures and materials.

Wright, D. (1999-2005). Car brake system FBD. University of Cambridge, Department of Engineering. Retrieved from http://www-mdp.eng.cam.ac.uk/web/library/enginfo/textbooks_dvd_only/DAN/brakes/vehicles/vehicles.html

Wang, J., & Zhang, C. (2021). Dynamic analysis of vehicle suspension systems under road disturbances. *Journal of Vehicle Dynamics*, 12(3), 245-260. https://www.researchgate.net/publication/262564822_Constructing_Equations_of_Motion_for_A_Vehicle_Rigid_Body_Model

Appendix 1 Highway rule for typical stopping Distances (NHTSA ,2023)

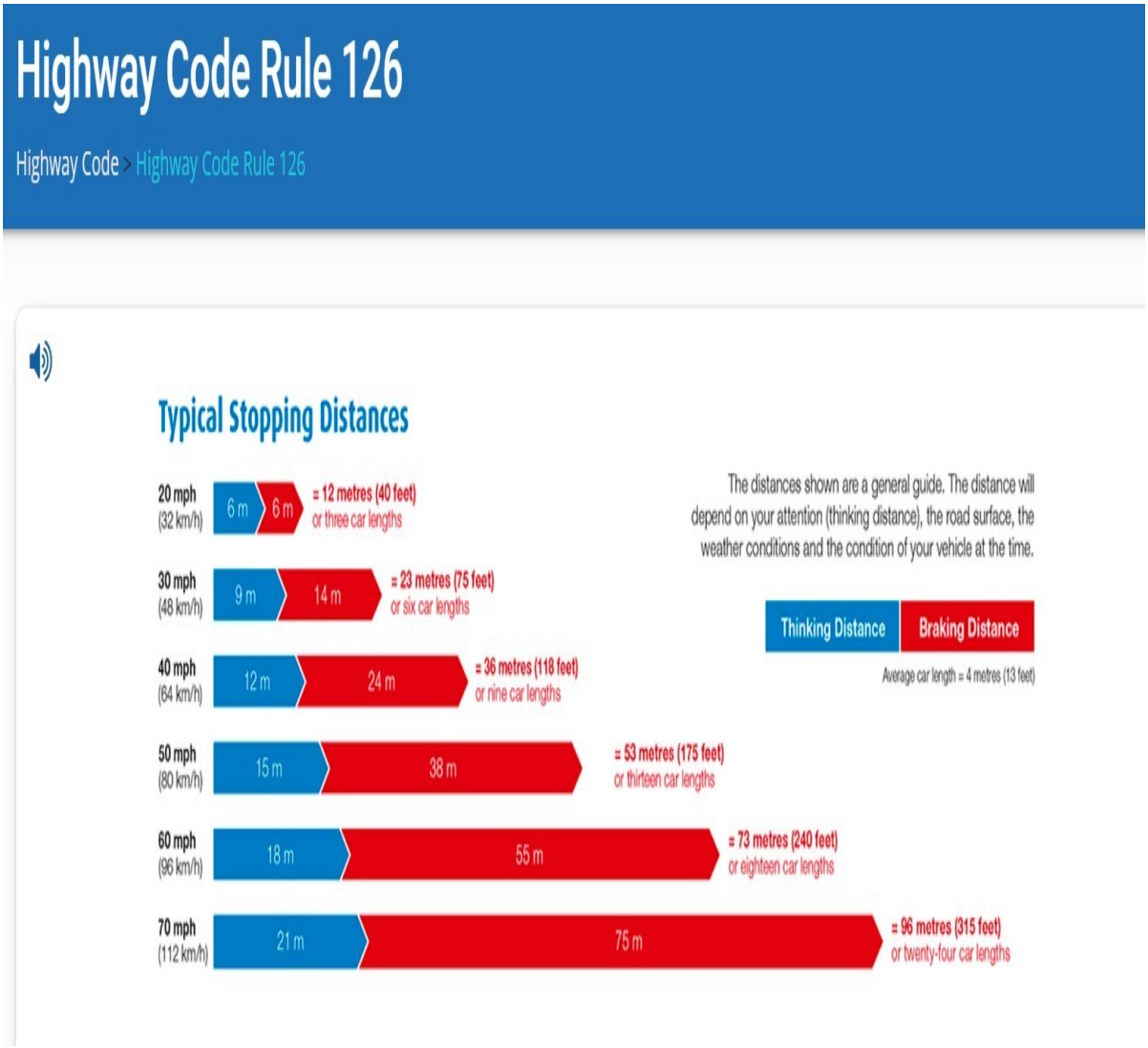

Appendix 2 Braking Acceleration of different Types of Cars (Smith, J., & Johnson, 2023)

Vehicle Type	Braking Acceleration (m/s^2)	Maximum Speed (km/h)	Source
Standard Passenger Car	5 - 8	100 - 140	Engineering Toolbox
Sports Cars	8 - 12	120 - 180	ResearchGate
SUVs	6 - 9	110 - 150	SAE International
City Buses	3 - 6	70 - 100	Automotive Engineering
Heavy Trucks	2 - 5	60 - 90	Omni Calculator
Race Cars	10 - 15	140 - 200	The Physics Classroom